Structural Determinants of Water Permeability through the Lipid Membrane

John C. Mathai,[1] Stephanie Tristram-Nagle,[2] John F. Nagle,[2,3] and Mark L. Zeidel[1]

[1]Department of Medicine, Beth Israel Deaconess Medical Center and Harvard Medical School, Boston, MA 02215
[2]Biological Physics Group, Department of Physics, and [3]Department of Biological Sciences, Carnegie Mellon University, Pittsburgh, PA 15213

Despite intense study over many years, the mechanisms by which water and small nonelectrolytes cross lipid bilayers remain unclear. While prior studies of permeability through membranes have focused on solute characteristics, such as size, polarity, and partition coefficient in hydrophobic solvent, we focus here on water permeability in seven single component bilayers composed of different lipids, five with phosphatidylcholine headgroups and different chain lengths and unsaturation, one with a phosphatidylserine headgroup, and one with a phosphatidylethanolamine headgroup. We find that water permeability correlates most strongly with the area/lipid and is poorly correlated with bilayer thickness and other previously determined structural and mechanical properties of these single component bilayers. These results suggest a new model for permeability that is developed in the accompanying theoretical paper in which the area occupied by the lipid is the major determinant and the hydrocarbon thickness is a secondary determinant. Cholesterol was also incorporated into DOPC bilayers and X-ray diffuse scattering was used to determine quantitative structure with the result that the area occupied by DOPC in the membrane decreases while bilayer thickness increases in a correlated way because lipid volume does not change. The water permeability decreases with added cholesterol and it correlates in a different way from pure lipids with area per lipid, bilayer thickness, and also with area compressibility.

INTRODUCTION

Water and solute permeability across lipid membranes have been extensively studied (Finkelstein, 1987; Haines, 1994; Xiang and Anderson, 1994; Jansen and Blume, 1995; Lande et al., 1995; Xiang and Anderson, 1995; Paula et al., 1996). The solubility-diffusion model, which treats the membrane as a homogeneous slab, is a widely accepted theory for transport of small molecules across membranes. It predicts that the permeability coefficient, P, of the molecule is proportional to the product of its partition coefficient, K, and diffusion coefficient, D_C in the membrane,

$$P = KD_C / d_C, \qquad (1)$$

and inversely proportional to the thickness of the membrane, d_C. A strong correlation of permeability with partition coefficient for different solutes has been shown in egg lecithin membranes, with permeability varying nearly over six orders of magnitude (Finkelstein, 1987).

However, many studies suggest that the solubility-diffusion model may be inadequate for describing passive membrane transport. For instance, the steep dependence of permeant size on permeability exhibited by biological membranes is not predicted by the solubility diffusion model (Lieb and Stein, 1986; Xiang and Anderson, 1994, 1998). Furthermore, highly ordered membranes were

shown to exhibit permeability values that deviate significantly from predictions made using the solubility diffusion model (Finkelstein, 1976; Brahm, 1983; Magin and Niesman, 1984; Xiang and Anderson, 1998).

The relative importance of the role of permeant partitioning vs. diffusion within the membrane has been studied experimentally and theoretically. The reduction in permeability of neutral small molecular weight solutes with increasing lipid chain order was attributed to resistance to solute diffusion within the membrane (Lieb and Stein, 1986; Lande et al., 1995). However, using a series of monocarboxylic acids in highly ordered membranes, the decreased solute permeability was thought to be due to reduced solute partitioning into the membrane (Xiang and Anderson, 1998). Molecular dynamics (MD) simulations (Marrink and Berendsen, 1994, 1996) support the earlier hypothesis (Diamond and Katz, 1974) that both the partition and diffusion coefficients depend continuously on position along the normal to the membrane, so there would be more than one "slab," even in a simplified scheme. Simulations based on scaled-particle

Correspondence to John C. Mathai: jmathai@bidmc.harvard.edu

Abbreviations used in this paper: CF, carboxyfluorescein; diC22:1PC, 1,2-dierucoyl-sn-glycero-3-phosphocholine; DLPC, 1,2-dilauroyl-sn-glycero-3-phosphocholine; DLPE, 1,2-dilauroyl-sn-glycero-3-phosphoethanolamine; DMPC, 1,2-dimyristoyl-sn-glycero-3-phosphocholine; DOPC, 1,2-dioleoyl-sn-glycero-3-phosphocholine; DOPS, 1,2-dioleoyl-sn-glycero-3-phospho-L-serine; MD, molecular dynamics; POPC, 1-palmitoyl-2-oleoyl-sn-glycero-3-phosphocholine.

theory suggest that the relative importance of partitioning and diffusion in the bilayer is dependent on solute size and also on lipid bilayer parameters (Mitragotri et al., 1999). Recent all atom simulation studies suggest that solute size dependence may be less for diffusion within the membranes compared with solute partitioning into the membrane (Bemporad et al., 2004).

Many studies have focused on the role of the size, shape, and polarity of the solute (Walter and Gutknecht, 1986). Relatively fewer, but quite notable, studies have considered the effect of individual lipids and lipid bilayer properties such as thickness, fluidity, area compressibility, free surface area, and lysis tension (Nagle and Scott, 1978; Xiang and Anderson, 1995, 1998; Mitragotri et al., 1999; Hill and Zeidel, 2000; Olbrich et al., 2000; Krylov et al., 2001; Mathai et al., 2001). In barrier membranes, the presence of specific lipids, such as cholesterol and sphingolipids, was shown to reduce water permeability (Lande et al., 1995). Furthermore, liposomes designed to mimic the inner and outer leaflets of the MDCK type-I apical membrane, a barrier epithelium, showed an 18-fold lower permeability for outer leaflet lipids compared with inner leaflet lipids (Hill and Zeidel, 2000; Krylov et al., 2001). In addition, reduction of water permeability has been correlated with decreased anisotropy of membranes (Lande et al., 1995; Negrete et al., 1996). Many of these studies suggest that tighter packing of lipids leads to a reduction of water permeability, as seems quite reasonable, but that does not address cases such as those studied in this paper, where the packing, as measured by the free volume, is essentially the same for different bilayers, but the permeability is not the same.

We therefore suggest that the influence on permeabilities of the basic structural parameters of the lipid bilayer, such as its area, thickness, volume, and its material properties, such as bending modulus, area compressibility modulus, and rupture tension, can benefit from further systematic study. Earlier studies on the influence of thickness of the membrane on permeability gave conflicting results as the lipids and methods used were different (Jansen and Blume, 1995; Paula et al., 1996). Furthermore the relative influence of the head group region and hydrocarbon region on the overall process of permeation is still unclear. In this study we have measured the water permeability of seven single component lipid systems comprised of various headgroups, chain lengths, and unsaturation. We have then examined the water permeability for correlations with various measured physical parameters of the lipids, such as area/lipid, hydrocarbon thickness, bending modulus, and compressibility modulus. Our results suggest that the rate-limiting step for water permeation is mainly determined by the area/lipid, and the contribution of thickness is secondary, as is discussed in detail in the following theoretical companion paper (see Nagle et al. on p. 77).

Furthermore, the permeability with added cholesterol continues to correlate with area per lipid, but with a significant difference compared with single component lipid bilayers.

MATERIALS AND METHODS

All chemicals were purchased from Sigma-Aldrich and were of the highest quality commercially available. The following lipids were purchased from Avanti Lipids in powdered form, 1-palmitoyl-2-oleoyl-*sn*-glycero-3-phosphocholine (POPC); 1,2-dioleoyl-*sn*-glycero-3-phosphocholine (DOPC); 1,2-dioleoyl-*sn*-glycero-3-phospho-L-serine (DOPS); 1,2-dimyristoyl-*sn*-glycero-3-phosphocholine (DMPC); 1,2-dilauroyl-*sn*-glycero-3-phosphocholine (DLPC); 1,2-dilauroyl-*sn*-glycero-3-phosphoethanolamine (DLPE); 1,2-dierucoyl-*sn*-glycero-3-phosphocholine (diC22:1PC).

Preparation of Unilamellar Liposomes
Lipid (5 mg) was weighed into a glass vial and dissolved in 1:2 chloroform–methanol solution. For DOPC samples with cholesterol, cholesterol was dissolved in chloroform and appropriate amounts of this solution were pipetted into the DOPC solution. The solvent was evaporated under nitrogen at 40°C and residual solvent was removed under vacuum overnight. The dried lipids were hydrated in carboxyfluorescein (CF) buffer (100 mM NaCl, 50 mM sucrose, 10 mM of fluorescent probe 5-6 CF and 20 mM MOPS, pH 7.4) at room temperature for 30 min. The lipid solution was vortexed for 1 min and briefly probe sonicated for 30–60 s at a low setting of 5 mW (Virsonic 60, The Viritis Company Inc.). This lipid solution was extruded 21 times through a 200-nm nucleopore filter by using the Avanti mini-extruder assembly. Extravesicular CF was removed by passing the solution through a Sephadex PD-10 desalting column (Amersham) and the liposomes were collected in the void volume. DMPC lipids were hydrated at 30°C and all operations on it, including the column elution work, were done at that temperature to avoid the liposomes going through the main transition at 24.0°C. Phosphatidylethanolamines form stable liposomes in conditions of either low ionic strength or high pH (Allen et al., 1990). For this reason a buffer solution of 100 mM NaCl and 10 mM Tris-HCl at pH 9.3 was used for preparation of DLPE liposomes. DLPE lipids have a transition temperature at 29.0°C, hence all operations on it were performed at 35.0°C. The size of the vesicles was measured by laser light scattering using a DynaPro particle sizer. The average diameter of the vesicles was in the range of 140–160 nm.

Permeability Measurements
Osmotic permeability for most samples was measured as described earlier (Lande et al., 1995). In brief, the unilamellar vesicles were abruptly subjected to a 50% increase of external osmotic pressure in an Applied Photophysics (SX.18 MV) stopped-flow device. The exit of water due to the osmotic gradient results in a decrease of liposomal volume, which is measured by the self-quenching of entrapped carboxyfluorescein. The time-dependent decrease in fluorescence was averaged for 8–12 time traces and fitted to a single exponential curve as shown in Fig. 1 A for DOPC. The osmotic water permeability, P_f, was calculated by comparing the single-exponential time constants fitted to a family of simulated curves generated using the water permeability equation in which P_f was varied to that obtained experimentally. MathCad was used to numerically integrate the water permeability equation obtained from Fick's law:

$$\frac{dV_r(t)}{dt} = P_f \times SAV \times V_w \times \left(\frac{C_{in}}{V_r(t)} - C_{out} \right), \qquad (2)$$

where $V_r(t)$ is the relative volume of the vesicle at time t (i.e., volume at time t, divided by the initial volume), P_f (cm/s) is the osmotic water permeability coefficient, SAV is the surface area to volume ratio of a vesicle, C_{in} and C_{out} are initial solute concentrations inside and outside the vesicle, respectively, and V_W is the volume of a water molecule.

Liposomes prepared from DLPC lipids did not entrap CF well and hence light scattering at 600 nm was used to measure their volume change as shown in Fig. 1 B. Light scattering measurements have a lower sensitivity compared with fluorescence-based techniques in measuring volume change. However, this limitation is overcome by increasing the amount of lipids used per measurement and both fluorescence and light scattering measurements report similar rates of volume change for any lipid. Light scattering was also used to measure the volume changes of DLPE liposomes.

All water permeability measurements were done within 120 min of sample preparation and at 30°C, the temperature at which structural studies were performed, with the exception of DLPE liposomes, which was measured at 35°C, at which its structural parameters were also measured (McIntosh and Simon, 1986).

Structural Measurements

Structural results for the seven single component lipid bilayers were obtained previously (see references in Table I). We will focus here on the modifications required for the new results for cholesterol in DOPC.

A stock solution of DOPC (Avanti Polar Lipids, Inc., lot no. 181PC-211) was prepared from dry powder and HPLC chloroform (Fisher Scientific) and stored at -20°C. The concentration of the stock solution (0.105 M) was verified by phosphate assay (Kingsley and Feigenson, 1979). Cholesterol lot CH-800-MA7 liter from Nuchek labs was also stored as a stock solution (0.0431 M) in chloroform at -20°C. Precise quantities of these stock solutions were added to disposable glass culture tubes using the microliter PB600 repeating dispenser on a Hamilton syringe to obtain 4 mg total lipid with cholesterol mole fractions (cholesterol/(cholesterol + DOPC)) from 0.05 to 0.4. The DOPC was found to migrate as a single spot using thin layer chromatography (65/25/4) (chloroform/methanol/water, vol/vol/vol) before and after x-ray exposure.

Oriented samples were prepared as described previously (Tristram-Nagle et al., 1993; Tristram-Nagle, 2007) to produce a 10-μm-thick lipid film of 0.5 mm width on a silicon wafer (1.5 × 3 × 0.1 cm) with the bilayers' surface parallel to the substrate. Capillary samples were also prepared by hydrating the DOPC/cholesterol mixtures described above by adding excess Barnstead nanopure water (20:1 or 10:1, vol:vol) in small nalgene vials, vortexing, temperature cycling from -20°C to 60°C three times, and then loading into x-ray capillaries (Charles Supper). The capillary sample yields the fully hydrated D-spacing, which is the end point of the hydration experiment through the vapor for oriented samples (see Kučerka et al., 2005, for more details).

X-ray data were taken in several runs at the Cornell High Energy synchrotron Source (CHESS). For the best data taken at the G-1 station, the X-ray wavelength was $\lambda = 1.2474$ Å, selected using a multilayer monochromator (Osmic), which had 1.2% full-width at half-maximal energy dispersion. The beam was narrow (0.26 mm) to provide small angular divergence (1.4 × 10^{-4} radian) in the horizontal direction, which is essential for the analysis of the diffuse scattering which provides the data extending to $q_z = 0.93$ Å^{-1}. Data were collected in duplicate scans of 10 s (G1) using a Flicam charge-coupled device (CCD) with a 1024 × 1024 pixel array, each pixel having linear dimension 69.78 μm. Capillary samples at 30°C were measured using a microfocus Rigaku RUH3R rotating anode equipped with a Xenocs FOX2D focusing multilayer and the data were collected in 5 min on a Mercury CCD (Rigaku). Silver behenate (D = 58.367 Å) was used to calibrate the sample to detector distances (372 mm at CHESS and 202 mm at CMU).
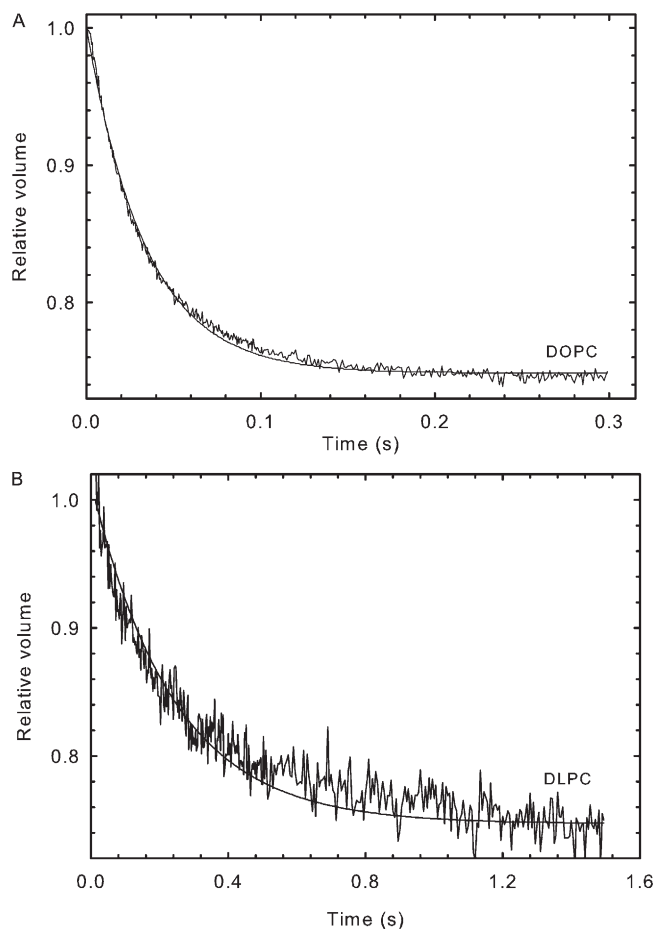

Figure 1. Water permeability measurement. Time trace of volume change of liposome measured by fluorescence quenching, DOPC (A), or light scattering, DLPC (B). Liposomes were subjected to a 50% increase in external osmotic pressure.

Analysis of the basic F(q_z) form factor data was performed as in Kučerka et al. (2005) using the H2 model of Klauda et al. (2006) with the cholesterol represented by an additional Gaussian in each monolayer. Fig. 2 illustrates the individual components that comprise the model. The hydrocarbon width d_C of the bilayer is determined from the Gibbs dividing surface for the lipid hydrocarbon tails (see Fig. 2). After fitting the model to the F(q_z) data, the area/lipid A_L was obtained as V_C/d_C where the volume of the hydrocarbon tails $V_C = V_L - V_H$ and $V_L = 1302$ Å^3 is the measured total volume of DOPC (Greenwood et al., 2006) and $V_H = 331$ Å^3 is the volume of the PC headgroup including the glycerol/carbonyl backbone (Tristram-Nagle et al., 2002).

The bending modulus K_C was obtained from the diffuse scattering data as previously described (Lyatskaya et al., 2001; Liu and Nagle, 2004). The area compressibility modulus K_A was calculated from K_C and d_C using the polymer brush equation $K_A = 24K_C/d_C^2$ (Rawicz et al., 2000).

RESULTS

Table I shows values of various measured physical parameters of lipid bilayers and their water permeability, and this information is plotted in Fig. 3. Fig. 3 A shows a good correlation of permeability with the lateral area A
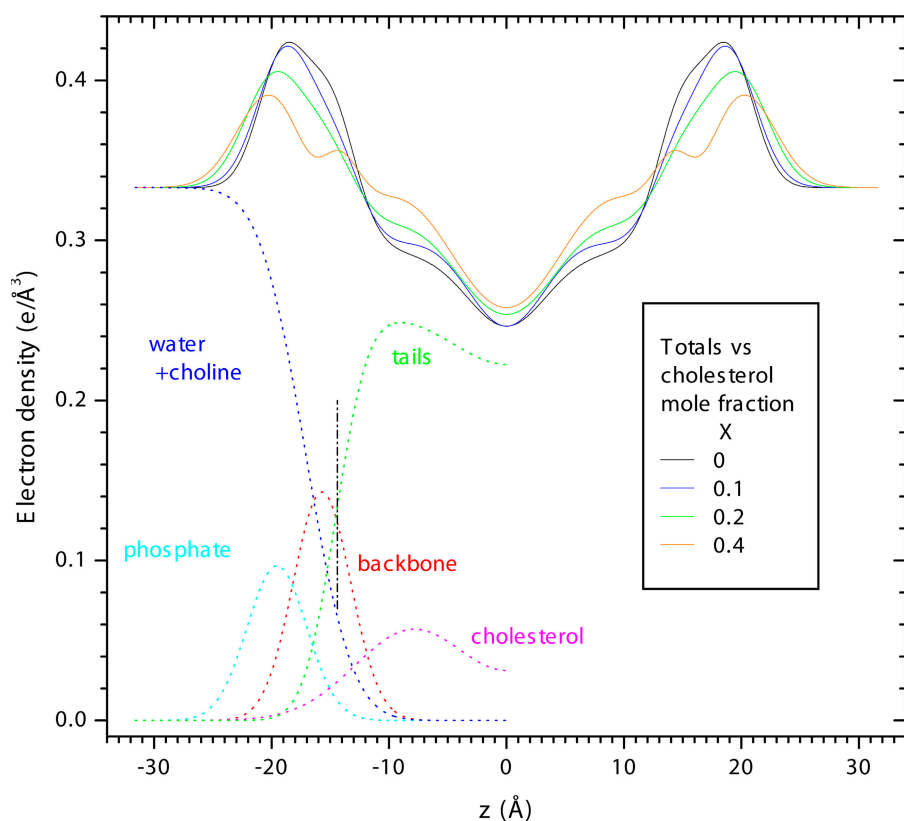
Figure 2. The dotted lines show the H2 model component contributions to the electron density for half the bilayer. These components include cholesterol, water, and various fragments of the lipid molecule; the backbone consists of both the glycerol and the carbonyls, and the choline is included with the water. The Gibbs dividing surface for the hydrocarbon tails, which gives d_C is indicated by the black vertical dot-dashed line. These dotted lines show the best fit of the H2 model to the $F(q_z)$ data obtained for X = 0.2 mol fraction cholesterol. Their sum is the total electron density shown by the solid green curve. The total electron densities shown for the other cholesterol concentrations indicate that the bilayer thickens with added cholesterol. The maxima correspond to the electron dense phosphate groups and the height of these maxima decrease as phospholipid is replaced by cholesterol.

per lipid molecule. By contrast, other parameters such as hydrocarbon thickness d_C, area compressibility K_A, and bending modulus K_C (Fig. 3, B–D), the volume per

methyl group V_{CH2} (see Table I), and the total lipid volume (not depicted) are not well correlated with water permeability. It may be noted that our measured values of
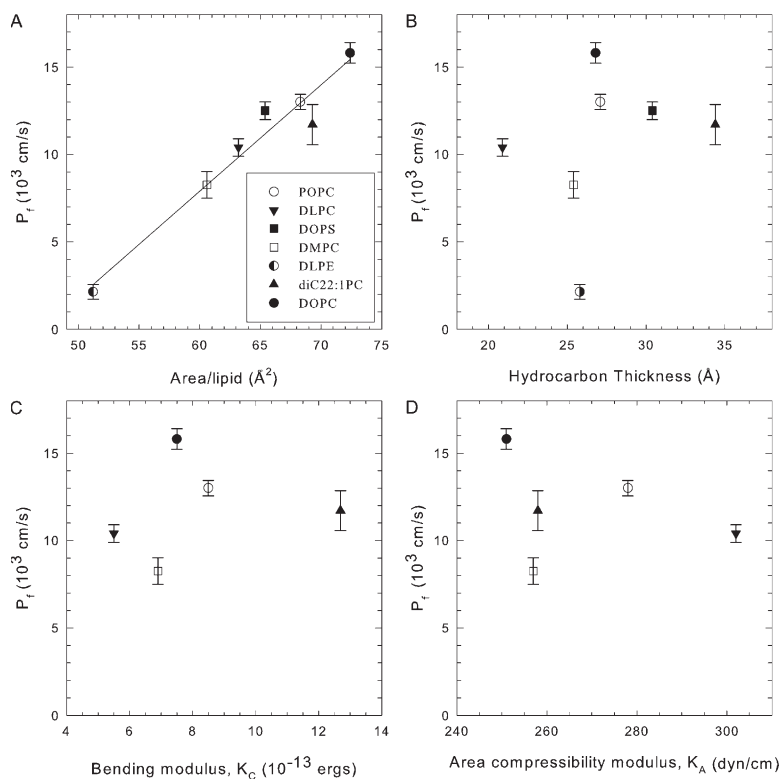

Figure 3. Correlation of osmotic water permeability with various structural parameters of lipid bilayers composed of a single kind of lipid. Water permeability correlates well with area/lipid of each molecule (A) while thickness (B), bending modulus (C), and compressibility (D) do not show any correlation. Each lipid is shown by a different symbol as shown in A. Compressibility and bending modulus data for DOPS and DLPE are not available and hence are omitted from the figure, C and D. These data are summarized in Table I.

TABLE I

Summary of Measured Lipid Parameters and Osmotic Water Permeability Values at 30°C

Lipid	Area/Lipid ($Å^2$)	Thickness ($Å$)	K_C (10^{-13} ergs)	K_A (dyn/cm)	V_{CH2} ($Å^3$)	P_f ($\times 10^{-3}$ cm/s)
DLPE[a,b]	51.2 ± 0.5	25.8	x	x	27.3	2.14 ± 0.41
DOPS[c]	65.4 ± 0.5	30.4	x	x	28	12.5 ± 0.50
DMPC[d]	60.6 ± 0.5	25.4	6.9	257	27.7	8.3 ± 0.76
DLPC[d]	63.2 ± 0.5	20.9	5.5	302	27.7	10.4 ± 0.50
POPC[e]	68.3 ± 1.5	27.1	8.5	278	27.6	13.0 ± 0.44
diC22:1PC[e]	69.3 ± 0.5	34.4	12.7	258	27.6	11.7 ± 1.15
DOPC[e]	72.4 ± 0.5	26.8	7.5	251	27.7	15.8 ± 0.58
+10% Ch	71.4 ± 1.0	27.2	6.9	223	27.7	14.5 ± 0.57
+20% Ch	67.5 ± 2.0	29	7.2	204	27.7	11.5 ± 0.58
+40% Ch	64.0 ± 1.0	30.6	7.3	187	27.7	6.8 ± 0.57

[a]35°C.

[b]McIntosh and Simon, 1986.

[c]Petrache et al., 2004.

[d]Kučerka et al., 2005.

[e]Kučerka et al., 2006.

K_C and our calculated values of K_A agree well with the values measured using the aspiration pipette technique (Rawicz et al., 2000) and that the differences do not improve the lack of correlation in Fig. 3 (C and D).

We also added varying amounts of cholesterol to DOPC lipid bilayers. Fig. 2 shows the electron density profiles for four concentrations of cholesterol and the values of the physical parameters are shown in Table I along with the corresponding water permeabilities. Fig. 4 A shows that the area/lipid A_L decreases as cholesterol content in the membrane increases, which is consistent with the well-known condensing effect of cholesterol (Edholm and Nagle, 2005). Furthermore the decrease in area/lipid correlates well with the decrease in water permeability. A comparison of slopes in the presence and absence of cholesterol (Fig. 5) shows that for a given area/lipid the decrease in permeability is greater in the presence of cholesterol than in its absence. Fig. 4 B shows that, unlike the behavior with single component lipid bilayers, there is a strong correlation of water permeability with thickness of the DOPC bilayer in presence of cholesterol. Fig. 4 C indicates little correlation of permeability with bending modulus, whereas area compressibility modulus K_A shows a good correlation in Fig. 4 D.

DISCUSSION

Water permeability values vary widely depending on the lipid composition, conditions employed, and the method of measurement. Our permeability value for DOPC lipid ($P_f = 0.0158$ cm/s) is close to the value of 0.015 cm/s obtained by Paula et al. (1996). Huster et al. (1997), using the ^{17}O NMR signal of water, monitored the exchange of water across various lipid membranes and reported a value of 0.012 cm/s at 25°C for DOPC

membrane vesicles, which extrapolates to 0.0142 cm/s at 30°C based on the activation energy. In contrast, using giant unilamellar vesicles and micropipette aspiration technique a value of 0.0042 cm/s at 21°C was given for DOPC membranes (Olbrich et al., 2000), which extrapolates to ~0.0067 cm/s at 30°C. Early studies of egg lecithin membranes showed an even smaller water permeability value of 0.0022 cm/s (Finkelstein, 1976); of the lipids we studied, egg lecithin is most similar to POPC membranes, which are monosaturated. Compared with relative differences in water permeability values, which have good reproducibility, absolute values of water permeability measured by different techniques and different laboratories can vary by an order of magnitude (Huster et al., 1997). Our water permeability measurements have been validated in planar bilayers using the membrane scanning microelectrode method (Krylov et al., 2001).

The very weak, essentially nonexistent, correlation of water permeability with membrane thickness for a variety of single component lipid bilayers with a range of different hydrocarbon thicknesses *dc* is surprising in view of the often accepted solubility-diffusion model which predicts the thickness dependence shown in Eq. 1. Our observation is similar to that seen experimentally for saturated lipids (Jansen and Blume, 1995). In contrast, using lipids that were monounsaturated in both lipid chains, it was concluded that there was a modest dependence of permeability on hydrocarbon thickness (Paula et al., 1996). Recent MD simulation studies using saturated PC lipids of various chain lengths also show a modest dependence on chain length (Sugii et al., 2005). Since the experimental details and the lipids used are different it is difficult to make a direct comparison. In order for Eq. 1 to fit our data would require that the partition coefficient *K* and/or the diffusion coefficient
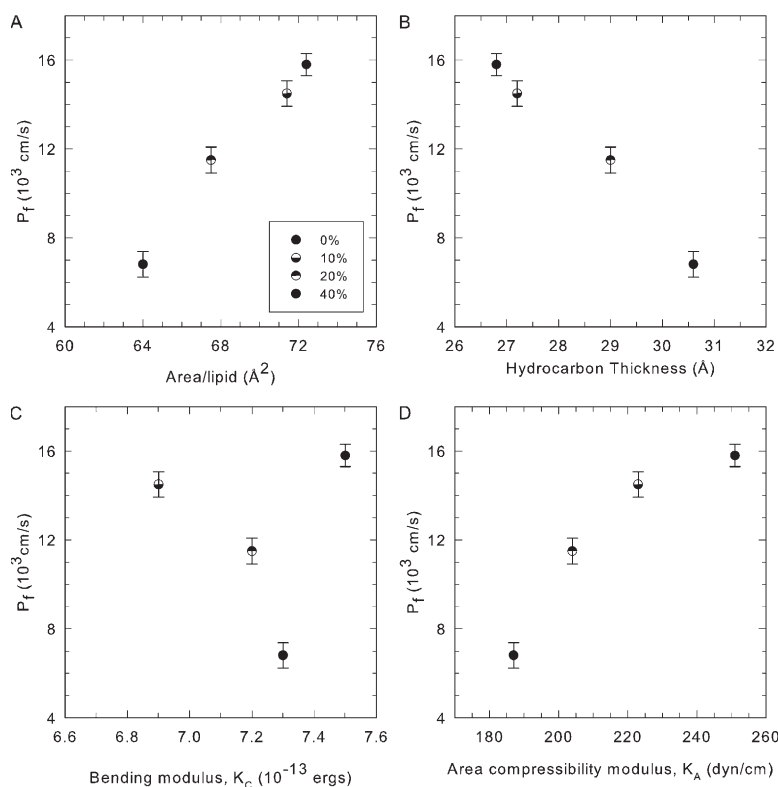
Figure 4. Water permeability of DOPC lipids in presence of increasing concentrations of cholesterol. Increasing concentrations of cholesterol (10, 20, and 40 mol%) result in a decrease in water permeability. This decrease correlates well with decrease in area per lipid (A) as well as increase in thickness (B) on addition of cholesterol. Water permeability shows a modest correlation with area compressibility (D) and none with bending modulus (C) of the membrane.

Dc within the hydrocarbon region depend strongly on the specific lipid. A dependence of K could be readily understood if the free volume of the hydrocarbon chains was different for the different lipids. However, the volume of the hydrocarbon chains per methylene is essentially identical for the five different PC lipids, so the free volume is also essentially the same, as indicated by the volume per methylene group shown in Table I. It is also unclear why the coefficient of diffusion Dc would depend significantly on the lipid when the hydrocarbon chains are all in the chain melted, fluid phase in which chain isomerization is fast on the picosecond time scale.

The strong correlation we find of water permeability with area per lipid suggests that rather than pursue refinements to the single slab solubility-diffusion model, other models may be warranted. Since the area per molecule is a surface property of lipid bilayers, this suggests that the interfacial region may constitute the rate-limiting step for water permeability. Based on studies of several solute permeabilities and partition coefficients (polar and nonpolar solvents) it was suggested that barrier domain is probably located closer to the membrane interface region (Xiang and Anderson, 1995, 1998). This leads back to a three slab model, a central slab for the hydrocarbon region and two interfacial slabs, similar to ones considered by Diamond and Katz (1974) and Zwolinski et al. (1949). The accompanying theoretical paper develops this idea by proposing an interfacial

steric blockage mechanism and by presenting detailed kinetic analysis to fit the proposed model to the present data.

While the previous discussion suggests that the solubility-diffusion model is deficient, it may still be of interest to explore the values that are required to make the central equation $P = KDc/d_C$ work for our data. Assuming $Dc = 2 \times 10^{-5}$ cm^2/s and using our values of d_C, the
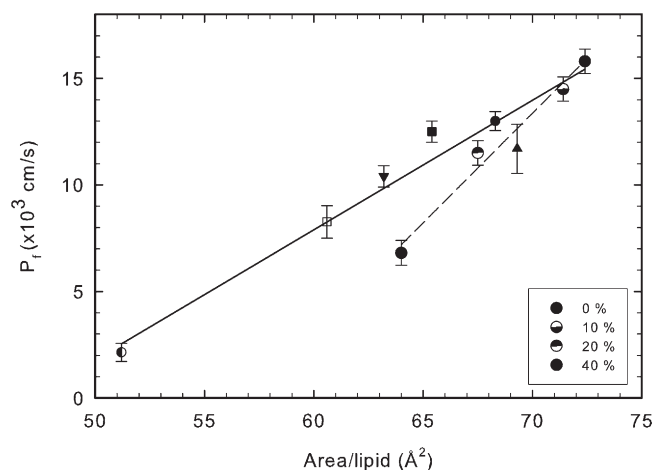

Figure 5. Effect of cholesterol on water permeability. A comparison of change in area/lipid and water permeability in absence and presence of cholesterol. Presence of cholesterol results in an increased slope of dP/dA.

K values calculated from Eq. 1 would be in the range of 0.3 to 2.1×10^{-4}. For comparison, the alkane solvents hexadecane and 1,9-decadiene, which some feel most closely resemble the hydrocarbon interior, have K values 0.59×10^{-4} and 1.2×10^{-4}, respectively (Xiang and Anderson, 1994). It might also be noted that some of the smaller values of P in the literature (Finkelstein, 1976; Walter and Gutknecht, 1986; Olbrich et al., 2000) would, for the same solvents, require unphysically large values of hydrocarbon thickness d_C.

Cholesterol is known to decrease water permeability across lipid membranes (Carruthers and Melchior, 1983; Lande et al., 1995), however its mechanism of action is not clear. We find that increasing amounts of cholesterol in the membrane cause a corresponding decrease in area occupied by the lipid and also cause a corresponding decrease in water permeability across these membranes. However, as shown in Fig. 5, this decrease in permeability versus area/lipid is greater upon addition of cholesterol to DOPC than upon varying the lipid in single component bilayers. This suggests that an additional factor other than area/lipid may be responsible for further decrease in water permeability in presence of cholesterol. This additional factor may be due to a decrease in partition coefficient K (Young and Dill, 1990). Increasing concentrations of cholesterol also increase the thickness of the hydrocarbon region as seen in Fig. 4 B, and the increased resistance to water permeability in presence of cholesterol shown in Fig. 5 may perhaps also be due partly to the combined effect of decreased area/lipid and increased thickness of the membrane.

It is important to understand that the correlation of water permeability with thickness seen in Fig. 4 B for cholesterol added to DOPC is consistent with the lack of correlation for different lipids seen in Fig. 3 B. It has been shown that the volume of DOPC does not change with added cholesterol (Greenwood et al., 2006), so any decrease in the area per lipid is directly correlated with an increase in the thickness of the bilayer. It is therefore not surprising that, unlike the case with different single component lipid bilayers, the permeability of DOPC bilayers with added cholesterol also correlates well with the bilayer thickness.

Material properties of the membrane such as its bending modulus and area compressibility modulus were measured and compared with its water permeability. We did not observe any correlation of water permeability with bending modulus, either in presence or absence of cholesterol. In contrast, area compressibility shows a modest correlation with permeability, but only as a function of added cholesterol as shown in Fig. 4. The anomalous peak in the passive permeability of sodium ions around the phase transition temperature was shown to be proportional to lateral compressibility of the membrane, which also has a peak near higher order phase transitions (Nagle and Scott, 1978), but the temperatures

for the water permeability data in this study were far enough from the transition temperatures that one would not expect a similar effect. In a study of polyunsaturated PC membranes comprised of equal chain lengths of 18 carbons, membranes with low values of lysis tension showed higher water permeability (Olbrich et al., 2000), suggesting that there may be an additional correlation between lysis tension and area per molecule A.

In summary we have found that water permeability (P_f) across seven single component lipid membrane systems correlates well with area A occupied by the lipid, irrespective of chain length, saturation, or composition of the headgroup. These experimental results have inspired the detailed theory in the accompanying paper that is based on the idea that the area that is not sterically blocked by the head group may be the dominant determinant for water permeability. We also confirm that P_f decreases when cholesterol is added to DOPC lipid bilayers and we obtain structural data that indicates that the decrease is also well correlated with area, although the rate of decrease dP/dA is greater than for single component bilayers. It remains to be explored if permeability of other small molecular weight solutes and gases across various lipid membranes is also strongly correlated with A.

REFERENCES

Allen, T.M., K. Hong, and D. Papahadjopoulos. 1990. Membrane contact, fusion, and hexagonal (HII) transitions in phosphatidylethanolamine liposomes. *Biochemistry.* 29:2976–2985.

Bemporad, D., C. Luttmann, and J.W. Essex. 2004. Computer simulation of small molecule permeation across a lipid bilayer: dependence on bilayer properties and solute volume, size, and cross-sectional area. *Biophys. J.* 87:1–13.

Brahm, J. 1983. Permeability of human red cells to a homologous series of aliphatic alcohols. Limitations of the continuous flow-tube method. *J. Gen. Physiol.* 81:283–304.

Carruthers, A., and D.L. Melchior. 1983. Studies of the relationship between bilayer water permeability and bilayer physical state. *Biochemistry.* 22:5797–5807.

Diamond, J.M., and Y. Katz. 1974. Interpretation of nonelectrolyte partition coefficients between dimyristoyl lecithin and water. *J. Membr. Biol.* 17:121–154.

Edholm, O., and J.F. Nagle. 2005. Areas of molecules in membranes consisting of mixtures. *Biophys. J.* 89:1827–1832.

Finkelstein, A. 1976. Water and nonelectrolyte permeability of lipid bilayer membranes. *J. Gen. Physiol.* 68:127–135.

Finkelstein, A. 1987. Water Movement through Lipid Bilayers, Pores, and Plasma Membranes: Theory and Reality. Wiley Interscience, New York. 228 pp.

Greenwood, A.I., S. Tristram-Nagle, and J.F. Nagle. 2006. Partial molecular volumes of lipids and cholesterol. *Chem Phys. Lipids.* 143:1–10.

Haines, T.H. 1994. Water transport across biological membranes. *FEBS Lett.* 346:115–122.

Hill, W.G., and M.L. Zeidel. 2000. Reconstituting the barrier properties of a water-tight epithelial membrane by design of leaflet-specific liposomes. *J. Biol. Chem.* 275:30176–30185.

Huster, D., A.J. Jin, K. Arnold, and K. Gawrisch. 1997. Water permeability of polyunsaturated lipid membranes measured by ^{17}O NMR. *Biophys. J.* 73:855–864.

Jansen, M., and A. Blume. 1995. A comparative study of diffusive and osmotic water permeation across bilayers composed of phospholipids with different head groups and fatty acyl chains. *Biophys. J.* 68:997–1008.

Kingsley, P.B., and G.W. Feigenson. 1979. The synthesis of a perdeuterated phospholipid: 1,2-dimyristoyl-sn-glycero-3-phosphocholine-d72. *Chem. Phys. Lipids.* 24:135–147.

Klauda, J.B., N. Kučerka, B.R. Brooks, R.W. Pastor, and J.F. Nagle. 2006. Simulation-based methods for interpreting x-ray data from lipid bilayers. *Biophys. J.* 90:2796–2807.

Krylov, A.V., P. Pohl, M.L. Zeidel, and W.G. Hill. 2001. Water permeability of asymmetric planar lipid bilayers: leaflets of different composition offer independent and additive resistances to permeation. *J. Gen. Physiol.* 118:333–340.

Kučerka, N., Y. Liu, N. Chu, H.I. Petrache, S. Tristram-Nagle, and J.F. Nagle. 2005. Structure of fully hydrated fluid phase DMPC and DLPC lipid bilayers using X-ray scattering from oriented multilamellar arrays and from unilamellar vesicles. *Biophys. J.* 88:2626–2637.

Kučerka, N., S. Tristram-Nagle, and J.F. Nagle. 2006. Closer look at structure of fully hydrated fluid phase DPPC bilayers. *Biophys. J.* 90:L83–L85.

Lande, M.B., J.M. Donovan, and M.L. Zeidel. 1995. The relationship between membrane fluidity and permeabilities to water, solutes, ammonia, and protons. *J. Gen. Physiol.* 106:67–84.

Lieb, W.R., and W.D. Stein. 1986. Transport and Diffusion Across Cell Membranes. W.D. Stein, editor. Academic Press Inc., Orlando, FL. 685 pp.

Liu, Y., and J.F. Nagle. 2004. Diffuse scattering provides material parameters and electron density profiles of biomembranes. *Phys. Rev. E Stat. Nonlin. Soft. Matter Phys.* 69:040901.

Lyatskaya, Y., Y. Liu, S. Tristram-Nagle, J. Katsaras, and J.F. Nagle. 2001. Method for obtaining structure and interactions from oriented lipid bilayers. *Phys. Rev. E Stat Nonlin. Soft. Matter Phys.* 63:011907.

Magin, R.L., and M.R. Niesman. 1984. Temperature-dependent permeability of large unilamellar liposomes. *Chem Phys. Lipids.* 34:245–256.

Marrink, S.J., and H.J.C. Berendsen. 1994. Simulation of water transport through a lipid membrane. *J. Physiol. Chem.* 98:4115–4168.

Marrink, S.J., and H.J.C. Berendsen. 1996. Permeation process of small molecules across lipid membranes studied by molecular dynamics simulations. *J. Physiol. Chem.* 100:16729–16738.

Mathai, J.C., G.D. Sprott, and M.L. Zeidel. 2001. Molecular mechanisms of water and solute transport across archaebacterial lipid membranes. *J. Biol. Chem.* 276:27266–27271.

McIntosh, T.J., and S.A. Simon. 1986. Area per molecule and distribution of water in fully hydrated dilauroylphosphatidylethanolamine bilayers. *Biochemistry.* 25:4948–4952.

Mitragotri, S., M.E. Johnson, D. Blankschtein, and R. Langer. 1999. An analysis of the size selectivity of solute partitioning, diffusion, and permeation across lipid bilayers. *Biophys. J.* 77:1268–1283.

Nagle, J.F., and H.L. Scott Jr. 1978. Lateral compressibility of lipid mono- and bilayers. Theory of membrane permeability. *Biochim. Biophys. Acta.* 513:236–243.

Nagle, J.F., J.C. Mathai, M.L. Zeidel, and S. Tristam-Nagle. 2007. Theory of passive permeability through lipid bilayers. *J. Gen. Physiol.* 131:77–85.

Negrete, H.O., R.L. Rivers, A.H. Goughs, M. Colombini, and M.L. Zeidel. 1996. Individual leaflets of a membrane bilayer can independently regulate permeability. *J. Biol. Chem.* 271:11627–11630.

Olbrich, K., W. Rawicz, D. Needham, and E. Evans. 2000. Water permeability and mechanical strength of polyunsaturated lipid bilayers. *Biophys. J.* 79:321–327.

Paula, S., A.G. Volkov, A.N. Van Hoek, T.H. Haines, and D.W. Deamer. 1996. Permeation of protons, potassium ions, and small polar molecules through phospholipid bilayers as a function of membrane thickness. *Biophys. J.* 70:339–348.

Petrache, H.I., S. Tristram-Nagle, K. Gawrisch, D. Harries, V.A. Parsegian, and J.F. Nagle. 2004. Structure and fluctuations of charged phosphatidylserine bilayers in the absence of salt. *Biophys. J.* 86:1574–1586.

Rawicz, W., K.C. Olbrich, T. McIntosh, D. Needham, and E. Evans. 2000. Effect of chain length and unsaturation on elasticity of lipid bilayers. *Biophys. J.* 79:328–339.

Sugii, T., S. Takagi, and Y. Matsumoto. 2005. A molecular-dynamics study of lipid bilayers: effects of the hydrocarbon chain length on permeability. *J. Chem. Phys.* 123:18471–18474.

Tristram-Nagle, S. 2007. Preparation of oriented, fully hydrated lipid samples for structure determination using X-ray scattering. *In* Methods in Molecular Biology: Methods in Membrane lipids. A.M. Dopico, editor. Humana Press Inc, Totowa, NJ. 63–75.

Tristram-Nagle, S., R. Zhang, R.M. Suter, C.R. Worthington, W.J. Sun, and J.F. Nagle. 1993. Measurement of chain tilt angle in fully hydrated bilayers of gel phase lecithins. *Biophys. J.* 64:1097–1109.

Tristram-Nagle, S., Y. Liu, J. Legleiter, and J.F. Nagle. 2002. Structure of gel phase DMPC determined by X-ray diffraction. *Biophys. J.* 83:3324–3335.

Walter, A., and J. Gutknecht. 1986. Permeability of small nonelectrolytes through lipid bilayer membranes. *J. Membr. Biol.* 90:207–217.

Xiang, T.X., and B.D. Anderson. 1994. The relationship between permeant size and permeability in lipid bilayer membranes. *J. Membr. Biol.* 140:111–122.

Xiang, T.X., and B.D. Anderson. 1995. Phospholipid surface density determines the partitioning and permeability of acetic acid in DMPC:cholesterol bilayers. *J. Membr. Biol.* 148:157–167.

Xiang, T.X., and B.D. Anderson. 1998. Influence of chain ordering on the selectivity of dipalmitoylphosphatidylcholine bilayer membranes for permeant size and shape. *Biophys. J.* 75:2658–2671.

Young, L.R.D., and K.A. Dill. 1990. Partitioning of nonpolar solutes into bilayers and amorphous n-alkanes. *J. Physiol. Chem.* 96:801–809.

Zwolinski, B.J., H. Eyring, and C.E. Reese. 1949. Diffusion and membrane permeability. I. *J. Physiol. Colloid. Chem.* 53:1426–1453.